

LOAN COPY

UILU-ENG 73 6010

T.&A.M. REPORT NO.364

CORRELATION BETWEEN FATIGUE CRACK PROPAGATION AND LOW CYCLE FATIGUE PROPERTIES

by

Saurindranath Majumdar

JoDean Morrow

Sponsored by

Advanced Research Projects Agency

ARPA Order No. 2169

The views and conclusions contained in this document are those of the authors and should not be interpreted as necessarily representing the official policies, either expressed or implied of the Advanced Research Projects Agency or the U.S. Government.

**DEPARTMENT OF THEORETICAL AND APPLIED MECHANICS
UNIVERSITY OF ILLINOIS
URBANA, ILLINOIS**

COLLEGE OF ENGINEERING DOCUMENTS OFFICE
UNIVERSITY OF ILLINOIS
112 ENGINEERING HALL
URBANA, ILLINOIS 61801

SUMMARY

Fatigue crack propagation is treated as a succession of fatigue crack initiation events. The cyclic stress and strain experienced by each element ahead of the crack tip is computed by means of an elastic-plastic analysis of the crack tip region. The attendant cumulative fatigue damage is computed in terms of low cycle fatigue properties of the metal. This permits a correlation to be made between the fatigue crack propagation resistance of a metal and its resistance to fatigue as measured on smooth specimens.

Over a limited range, a log-log plot of the fatigue crack propagation rate, da/dN , versus the stress intensity range, ΔK , is usually found to be nearly linear and may be written in the form: $da/dN = A(\Delta K)^p$. It is found in this investigation that the coefficient, A , and the exponent, p , depend upon the types of assumptions used in the analysis to deal with the stress-strain singularity at the notch tip. If the crack tip radius is assumed to be blunted to the value of the crack opening displacement, p is found to be equal to two and A is only a function of the low cycle fatigue properties of the material. If the additional assumption is made that each metal has a microstructure size, ρ^* , below which continuum mechanics solutions are not applicable, the coefficient A is found to be a function of ΔK . This causes a significant deviation from the log-log linear relationship usually assumed to exist between da/dN and ΔK . The analysis indicates that at small values of ΔK the crack propagation rate rapidly decreases until it approaches zero at a "threshold" value of ΔK .

Fatigue crack propagation data for eight steels from Barsom's work are compared with predictions from the analysis using low cycle fatigue properties and values of ρ^* based on Gurland's study of the dimension of the microstructural elements responsible for strengthening in steels. In all cases the estimate of da/dN was within a factor of two of the measured values.

ACKNOWLEDGMENT

This study was performed in the H. F. Moore Fracture Research Laboratory of the Department of Theoretical and Applied Mechanics, University of Illinois at Urbana-Champaign. Support was provided by the Advanced Research Projects Agency of the Department of Defense under U. S. Department of the Army No. DAHC-15-72-G-10, ARPA order No. 2169.

Professor H. T. Corten, Principal Investigator, and Professors G. M. Sinclair and H. R. Jhansale, Faculty Associates, contributed to this research through helpful discussions and critical review of the manuscript. Dr. R. H. Sailors was most helpful in directing our attention to the appropriate literature on the microstructural characteristics of steels.

LIST OF SYMBOLS

a	Semi-crack length
b, c	Fatigue strength and ductility exponents
c'	Modified fatigue ductility exponent
n, n'	Strain hardening exponent, Cyclic value
p	Fatigue crack propagation exponent
x, y	Coordinates along and normal to crack length
A	Fatigue crack propagation coefficient
COD	Crack opening displacement at maximum load
E, G	Young's modulus and shear modulus
K_{Ic}	Plane strain critical stress intensity factor
N, N_f, N_t	Cycles, Cycles to failure, Transition fatigue life
R_p	Reversed plastic zone size
λ	Mean free path as defined by Gurland
ρ	Effective crack tip radius
ρ^*	Microstructure size related to λ
σ, ϵ	Normal stress and normal strain
σ'_f, ϵ'_f	Fatigue strength and ductility coefficients
σ_y	Monotonic yield strength
σ'_y, ϵ'_y	Cyclic uniaxial yield strength and yield strain
τ, γ	Shear stress and shear strain
τ_o, γ_o	Shear yield strength and yield strain
ΔK	Stress intensity factor range (defined as $\Delta S\sqrt{\pi a}$)
ΔK_{th}	Threshold stress intensity factor range
ΔS	Nominal stress range
$\Delta \epsilon_p, \Delta \epsilon_e$	Plastic strain range and elastic strain range
$\Delta \sigma, \Delta \epsilon$	Normal stress range and normal strain range
$\Delta \tau, \Delta \gamma$	Shear stress range and shear strain range

INTRODUCTION

The problem of plane strain fatigue crack propagation has been the subject of extensive study over the last decade. In 1961 Paris, Gomez and Anderson (1) suggested a correlation between the fatigue crack propagation rate and the range of the applied stress intensity factor. Experimental results are now generally presented in a form similar to Fig. 1 which is a schematic log-log plot of the crack propagation rate, da/dN , as a function of the stress intensity factor range, ΔK , (defined as $\Delta S \sqrt{\pi a}$). Most metals appear to exhibit a "threshold" value of ΔK , below which fatigue cracks do not measurably propagate. Above the threshold value there is usually an intermediate range of ΔK over which da/dN is nearly linearly related to ΔK on a log-log basis. At higher ranges, the crack propagation rate increases rapidly as the maximum stress intensity approaches the critical value of K_{Ic} . The crack propagation rate in the intermediate zone is related to the range of stress intensity by the following equation:

$$\frac{da}{dN} = A(\Delta K)^p \quad (1)$$

where A and p are experimentally determined constants.

A variety of tests (2-6) have shown that for most metals the exponent p in Eq. (1) usually varies between two and four, though values as large as eight have occasionally been reported. This makes Eq. (1) dimensionally cumbersome. Depending on the value of the exponent, p , the constant, A , will have different dimensions.

Using continuum mechanics variables in a dimensional analysis, Liu (7) has shown that the exponent p in Eq. (1) should be two. The experimentally observed deviation of p from two can be accommodated within the framework

of continuum mechanics by permitting the coefficient, A , in Eq. (1) to be a function of ΔK . This requires the introduction of a "length parameter" which may be regarded as a measure of the microstructural dimension in the metal below which usual continuum mechanics does not apply. In this paper a dimensionally compatible relationship is proposed between ΔK and da/dN which has been derived by analyzing a simple fatigue crack propagation model similar to that proposed by Liu and Iino (8).

There are practical as well as theoretical reasons for attempting to relate fatigue crack propagation to other material properties via the analysis of a model such as used here. A significant problem facing materials engineers is the selection of materials to resist fatigue crack propagation at intermediate and low stresses. Few guidelines are currently available for choosing the most crack resistant metal from a group of candidates short of conducting fatigue crack propagation tests. From this point of view, it would be desirable to relate A and p in Eq.(1) to other known mechanical properties of metals.

Review of Fatigue Crack Propagation Models

Several investigators have attempted to correlate fatigue crack propagation with other mechanical properties. For example, Tomkins (9) has analyzed fatigue crack propagation using the plastic cohesive stress approach of Dugdale (10) and concluded that fatigue crack growth rate is basically dependent upon the cyclic stress-strain characteristics of materials. Hickerson and Hertzberg (11) have considered the correlation of fatigue crack growth resistance of materials with other mechanical properties and found the cyclic strain hardening exponent, cyclic yield strength, and elastic modulus to be important parameters.

A number of continuum mechanics models of fatigue crack propagation have been analyzed in the past. For example, McClintock (12) proposed a fatigue crack propagation model on the basis that fracture at the crack tip occurs whenever the accumulated average plastic strain reaches a critical value in a small sector of material just ahead of the crack tip. The radius of the sector which McClintock called the structure size, was interpreted as the smallest region to which a macroscopic fracture criterion can be applied (he used a value of 2×10^{-4} in.). From his damage analysis, McClintock concluded that the crack propagation rate is proportional to the square of the plastic zone size.

Rice (13) has considered fatigue crack growth based on the plasticity model of slip ahead of the crack. Tracing the deformation history of a particular point after it is encompassed by the plastic zone until the crack tip advances to the point, separation was assumed to occur when the total absorbed hysteresis energy equalled a postulated critical value per unit area. He obtained a relation similar to Eq. (1) with $p = 4$ but his model does not provide a direct interpretation of the physical meaning of the critical hysteresis energy.

Using Neuber's rule (14), Weiss (15) derived a crack propagation law under the assumption that the incremental growth per cycle is equal to the distance over which the strain ahead of the crack tip exceeds some critical value. The analysis of Weiss included a microstructure length constant, ρ^* , as introduced by Neuber to analyze the fatigue behavior of sharp notches.

Liu and Iino (8) proposed a model in which it is assumed that the points ahead of the crack tip constitute a set of uniaxial fatigue specimens. The propagation of a fatigue crack is assumed to be due to the successive fatigue failure of each of these imaginary specimens. By postulating equal

crack advance per cycle and experimentally measuring the plastic zone size and the strain distribution ahead of the crack tip, they derived an equation similar to Eq. (1) with $p = 2$.

Fleck and Anderson (16) have analyzed a model similar to that used by Liu and Iino (8). They used Rice's (13) discrete surface of slip or tensile yielding analysis (for a perfectly plastic material) to estimate the plastic zone size ahead of the crack tip. It was postulated that a fatigue element fails when the crack has progressed half way through the element. By suitably choosing the uniaxial material properties and the element size, Fleck and Anderson (17) obtained correlation between experimental data and their analysis for various metals.

Scope

The present paper adopts Liu's model, but instead of experimentally determining the plastic zone size and the strain distribution ahead of the crack, the analytical results obtained by Rice (18) are employed. In its simplest form, the analysis results in the exponent, p , of Eq. (1) being equal to two. The coefficient, A , can be calculated from the usual cyclic stress-strain and fatigue properties of uniaxial specimens of a given metal. Further, by introducing a microstructure size, ρ^* , into the analysis it is shown that a nonlinear relationship between $\log \Delta K$ and $\log da/dN$ may be obtained which quantitatively agrees with the trends in experimental data. The nonlinearity is achieved by keeping the power, p , equal to two while the coefficient, A , becomes a function of ΔK . Thus, the dimensionality of Eq. (1) is maintained.

DESCRIPTION OF THE FATIGUE CRACK PROPAGATION MODEL

Figure 2 shows the model to be analyzed and a schematic representation of the stress and strain history experienced by an element ahead of a propagating crack in a plate subjected to repeated tension so that ΔK is constant. Figure 3a depicts an essentially undamaged element ab at the reversed plastic zone boundary. Figure 3b shows the same element with the crack at a distance x from it. The damage experienced by element ab in one cycle at this location will be the same as experienced by element cd in Fig. 3a (assuming ΔK is constant). Thus, the cumulative damage required to cause fatigue failure of an element is equivalent to the sum of the damage experienced during one cycle by each element lying within the reversed plastic zone. Let $N_f(x)$ be the fatigue life of a specimen of the material subjected to constant cyclic strain equal to that which is present at a distance x from the crack tip. Using linear fatigue damage summation, failure of the element will occur when

$$1 = \sum_{x=0}^{R_p} \frac{1}{N_f(x)} \quad (2)$$

Assuming that ΔK is constant the crack advances in each cycle a constant amount, $\Delta x = da/dN$. Multiplying the left side of Eq.(2) by da/dN and the right side by Δx and approximating the sum by an integral:

$$\frac{da}{dN} = \int_0^{R_p} \frac{1}{N_f(x)} dx \quad (3)$$

Approximating the sum by an integral is equivalent to approximating the area under the step-like curve by the area under the smooth dotted curve in Fig. 3c.

MECHANICS AND FATIGUE

ANALYSIS OF THE CRACK TIP REGION

Rice (13, 18) considered a stationary crack loaded in antiplane shear (mode III) under small scale yielding in a material with the following shear stress-strain law:

$$\begin{aligned} \tau &= G\gamma & \text{for } \gamma \leq \gamma_0, \tau \leq \tau_0 \\ \tau &= \tau_0 (\gamma/\gamma_0)^n & \text{for } \gamma \geq \gamma_0, \tau \geq \tau_0 \end{aligned} \quad (4)$$

Assuming that the plastic strain components at each point within the plastic zone remain proportional to each other, Rice derived the following expressions for cyclic stress and strain ranges:

$$\Delta\tau = 2\tau_0 \left[\frac{\Delta K_{III}^2}{4(1+n) \pi \tau_0^2 x} \right]^{\frac{n}{1+n}} \quad (5)$$

$$\Delta\gamma = 2\gamma_0 \left[\frac{\Delta K_{III}^2}{4(1+n) \pi \tau_0^2 x} \right]^{\frac{1}{1+n}}$$

A similar analysis for tensile loading (mode I) is not available.

McClintock (12) has discussed the analogy between mode III and mode I for the case where displacements parallel to the crack are small compared to those normal to the crack surface. In the present study the above analogy will be used to approximate the stress and strain ranges ahead of a tensile crack in a material obeying the following cyclic stress-strain law:

$$\begin{aligned} \sigma &= E \epsilon & \text{for } \epsilon \leq \epsilon'_y \\ \sigma &= \sigma'_y (\epsilon/\epsilon'_y)^{n'} & \text{for } \epsilon \geq \epsilon'_y \end{aligned} \quad (6)$$

In terms of the product of stress and strain range, Eq. (5) reduces to

$$\Delta\sigma \Delta\epsilon = \frac{\Delta K^2}{(1 + n') \pi E x} \quad (7)$$

The reversed plastic zone size, R_p , and the crack opening displacement at maximum load, COD, are given by the following:

$$R_p = \frac{1}{4(1 + n')} \frac{\Delta K^2}{\pi \sigma_y'^2} \quad (8)$$

$$COD = \frac{2 \epsilon'_y \Delta K^2}{\pi \sigma_y'^2} \quad (9)$$

Even though the above equations are derived for a stationary crack, they will be assumed to hold for a propagating crack. The use of the fully stabilized cyclic stress-strain law may be justified, provided the crack propagation rate is slow enough that each point within the plastic zone spends sufficient number of cycles at each strain range to attain stable stress-strain behavior.

In order to compute the fatigue life of an element ahead of the crack tip subjected to a known stress-strain range, the following power functions will be used:

$$\Delta\sigma = 2 \sigma'_f (2N_f)^b \quad (10a)$$

$$\Delta\epsilon = 2 \epsilon'_f (2N_f)^c \quad (10b)$$

Note that in Eq. (10b) the fatigue life has been assumed to be related to the total strain range by a power function. In most materials, however,

the total strain range is related to the fatigue life by the following equation (Fig. 4):

$$\Delta\epsilon = \Delta\epsilon_p + \Delta\epsilon_e = 2\epsilon'_f (2N_f)^c + \frac{2\sigma'_f}{E} (2N_f)^b \quad (11a)$$

Equation (11a), in general, cannot be solved for the fatigue life explicitly and consequently a numerical method has to be adopted. On the other hand a closed form solution to the present problem may be obtained if the following approximations are made. The majority of the damage experienced by a fatigue element ahead of the crack occurs well inside the reversed plastic zone (17) where the plastic strain range is much larger than the elastic strain range. Consequently, in the low cycle (high strain) regime of fatigue, the fatigue life for a given strain range will lie between the following two power functions with slightly different exponents, c and c' , as defined in Fig. 4:

$$\Delta\epsilon \approx \Delta\epsilon_p = 2\epsilon'_f (2N_f)^c \quad (11b)$$

$$\Delta\epsilon \approx 2\epsilon'_f (2N_f)^{c'} \quad (11c)$$

The exponent c is the usual fatigue ductility exponent or the slope of the $\log \Delta\epsilon_p$ versus $\log 2N_f$ plot. A straight line on the log-log plot connecting the intercept at one reversal (the fatigue ductility coefficient, ϵ'_f) and the strain range at the transition fatigue life will have a slope of c' .

Note that Eq.(11b) always underestimates and Eq.(11c) always overestimates the fatigue life in the relevant range of the curve in Fig. 4. Thus the crack propagation analysis based on Eqs. (11b) and (11c) should bracket the results that would be obtained if the unabridged Eq. (11a) were used to compute fatigue lives.

Multiplying Eqs. (10a) and (10b) and equating the result to Eq. (7) gives the damage sustained in one cycle by an element at a distance x from the crack tip.

$$\frac{1}{N_f} = 2 \left[\frac{\Delta K^2}{4(1 + n') \pi E \sigma_f' \epsilon_f'} \right]^{\frac{-1}{b+c}} (x)^{\frac{1}{b+c}} \quad (12)$$

A disturbing aspect of Eq. (12) is that the integral in Eq. (3) is divergent for usual values of b and c . This singularity can be avoided by introducing crack tip blunting. At any instant the crack tip will have a finite radius that is approximately equal to half of the crack opening displacement. To treat this problem rigorously, a full nonlinear analysis is needed which unfortunately is not available. In the absence of such an analysis Rice's results are modified by translating the origin of the axes into the crack a distance of $COD/2$. In other words, x in Eq. (12) is replaced by $x + COD/2$. Substituting the modified form of Eq. (12) into Eq. (3) and using Eqs. (8) and (9) gives:

$$\frac{da}{dN} = \frac{-2(b+c)}{b+c+1} \left[\frac{\sigma_y'}{4(1 + n') \sigma_f' \epsilon_f'} \right]^{\frac{-1}{b+c}} \left\{ 1 - [4(1 + n') \epsilon_y']^{-\frac{b+c+1}{b+c}} \right\} \frac{\epsilon_y' \Delta K^2}{\pi \sigma_y'^2} \quad (13)$$

Since all terms in Eq. (13) except da/dN and ΔK are constants for a given metal, it may be written in a form similar to Eq. 1 with $p = 2$ as follows:

$$\frac{da}{dN} = A(\Delta K)^2 \quad (13a)$$

The coefficient A , is a function of the cyclic stress-strain and fatigue properties of the metal. In the derivation of Eq. (13), σ_y' , ϵ_y' and n' have been used to characterize the cyclic deformation resistance and σ_f' , ϵ_f' , b and c , the fatigue resistance of the metal.

INFLUENCE OF MATERIAL PROPERTIES ON THE COEFFICIENT OF EQ.(13)

Equation (13) requires the exponent of ΔK in Eq. (1) to be two and the coefficient A is expressed as a function of the cyclic stress-strain and fatigue properties of materials. For any fixed ΔK , the A 's are proportional to the rate of fatigue crack propagation for different metals. Thus the quantitative influence of these properties on fatigue crack propagation resistance may be evaluated by calculating their effect on the coefficient A .

For making such an evaluation, reference values for ϵ'_f , σ'_f , σ'_y , n' , b , c and E shown in Fig. 5 were chosen and each property in turn was varied keeping the others fixed.*

The effects of the various properties on the coefficient A are shown in dimensionless form in Fig. 5. Though the variation in one material property without accompanying variation in the others is highly unrealistic, these plots still serve to indicate how sensitive the coefficient A is to small changes in material properties. This helps separate those properties that need to be known accurately from those that need not be.

It is seen in Fig. 5 that the coefficient A is more sensitive to relative changes in fatigue strength coefficient (σ'_f), fatigue ductility coefficient and exponent (ϵ'_f and c) and elastic modulus (E) than to changes in other material properties. These four properties, therefore, have to be known more accurately than the rest for proper evaluation of fatigue crack resistance.

It is interesting to note that according to the present analysis, the cyclic yield strength (σ'_y) and the cyclic strain hardening exponent (n') appear to be of relatively minor importance in determining fatigue crack propagation resistance.

* The reference values in Fig. 5 were chosen to be representative of a slightly hardened structural steel.

EFFECT OF MICROSTRUCTURE SIZE

A microstructure size, ρ^* , may be incorporated in the analysis as follows. Assume there is a distance ρ^* ahead of the crack tip that is a function of the microstructure of the material within which the usual continuum mechanics approach is not meaningful. In other words, continuum analysis and bulk fatigue properties are applicable only from a distance ρ^* ahead of the crack tip, and Eq.(3) should be modified by changing the lower limit of the integral from 0 to ρ^* . The results will then be applicable provided the reversed plastic zone size R_p is large compared to ρ^* . Incorporating these modifications into the analysis Eq. (13) is altered as follows:

$$\frac{da}{dN} = \frac{-2(b+c)}{b+c+1} \left[\frac{\sigma'_y}{4(1+n')\sigma'_f \epsilon'_f} \right]^{\frac{-1}{b+c}} \left\{ \left[1 + \frac{2\rho^*}{COD} \right]^{\frac{b+c+1}{b+c}} - \left[4(1+n')\epsilon'_y \right]^{\frac{b+c+1}{b+c}} \right\} \frac{\epsilon'_y \Delta K^2}{\pi \sigma'^2_y} \quad (14)$$

The condition $R_p \gg \rho^*$ implies

$$\Delta K \gg 2(1+n')^{1/2} \sigma'_y \sqrt{\pi \rho^*} \quad (15)$$

Notice that for large enough load levels, COD will be large compared to ρ^* and Eq. (14) becomes the same as Eq. (13). For small loads where COD is of the order of ρ^* , Eq. (14) will give significant reduction in da/dN from Eq. (13). Thus, in general, the log da/dN versus log ΔK plot will be nonlinear and will asymptotically approach the linear relationship of Eq. (13) for large values of ΔK . At small ΔK 's the plastic zone size will approach the value of ρ^* which, according to this analysis, will arrest crack growth. Thus, the limiting value of ΔK from Eq. (15) may be regarded as an estimate of the threshold value, ΔK_{th} .

Figure 6 contains plots of ΔK versus da/dN for a typical steel (same properties as used as reference in Fig. 5) and for various values of

ρ^* . It may be observed that the effect of ρ^* is significant at low values of ΔK and tends to be less significant at higher values of ΔK . The fatigue crack growth resistance of any metal may then be thought of as consisting of two parts. Firstly, the fatigue crack growth resistance is controlled by the bulk low cycle fatigue properties and is given by Eq. (13). Secondly, an increase in resistance beyond that predicted by Eq. (13) is achieved by introducing the microstructure size, ρ^* . It is the latter effect that makes it necessary to select an exponent p of Eq. (1) that is greater than two in order to fit the power function to experimental data over a limited range of ΔK .

The physical interpretation of the microstructure size, ρ^* , is not clear. Some possibilities would include the distance between slip bands, grain size, carbide spacing, mean free ferrite path, and so on.

The effects of size or scale of the microstructure on the yield strength of steels have been studied in some detail. Recently, Gurland (19) has shown that in many steels of various microstructures, the yield strength can be expressed as a function of a microstructural parameter, λ , in a form similar to the Hall-Petch equation, i.e.:

$$\sigma_y = \sigma_o + k_y \lambda^{-1/2} \quad (16)$$

σ_o = Friction stress

k_y = Constant

$\lambda = \begin{cases} \text{Grain size in low carbon mild steels} \\ \text{Mean free path between cementite particles for spheroidic and tempered steels} \\ \text{Mean cell diameter in deformed pearlitic steels} \end{cases}$

When λ is interpreted as above, data for a variety of steels correlate well with a single Hall-Petch equation. For the purposes of the present paper ρ^* for steels will be approximated by λ .

COMPARISON OF EQ. (14) WITH BARSOM'S DATA ON STEEL

Published crack propagation data are seldom accompanied by cyclic or low cycle fatigue properties of the metals studied. To compare crack propagation data from the literature with Eq. (14), therefore requires that the appropriate mechanical properties first be estimated. Barsom's data (6) on fatigue crack propagation in steels were chosen for comparison with Eq. (14). The fatigue strength and ductility coefficients were approximated from the reported values of ultimate tensile strength and true fracture ductility (20). The fatigue ductility exponent, c , was approximated as -0.60 for the four soft steels and as -0.65 for the harder steels. The various properties assumed for computation are shown in Table I.

As mentioned before, ρ^* has been approximated by λ as given in Eq. (16). Gurland's (19) reported values for $\sigma_o = 10.5$ ksi and $k_y = 0.564$ ksi $\sqrt{\text{in}}$ were used in Eq. (16).

Figures 7 through 14 show the predicted values of crack propagation rate according to Eq. (14) together with Barsom's test data. The predicted values have been based on two values of c in Eq. (10b) as discussed earlier. For all practical purposes, Barsom's test data fall within the band of predicted values in all cases. Notice that the value of ρ^* for the high yield steels are on the average a factor of ten smaller than those for the low yield steels. Over the range of ΔK investigated by Barsom for the high yield strength steels, the effect of ρ^* is small. On the other hand, for the low yield strength steels the introduction of ρ^* gives excellent correlation with both the magnitude of the crack propagation rate and the slope of the $\log \Delta K - \log da/dN$ plots.

CONCLUDING REMARKS

Ignoring the effect of microstructure size, Eq. (13) gives the maximum potential rate of fatigue crack propagation for any given range of stress intensity factor, and the slope of the $\log \Delta K - \log da/dN$ plot is two. This maximum potential fatigue crack propagation rate is controlled by the bulk mechanical properties of the metal, particularly the fatigue ductility coefficient and exponent, the fatigue strength coefficient, and the elastic modulus. For this kind of fatigue crack resistance the yield strength is theoretically of little importance (Fig. 5).

By introducing a microstructure size into the analysis the crack propagation rate for any given stress intensity factor range is reduced, especially at intermediate to low values of stress intensity factor. The increase in fatigue crack propagation resistance is larger the larger the microstructure size (Fig. 6). In steels, a Hall-Petch type equation may be used for computing the relevant microstructure size from the yield strength. Since the microstructure size varies inversely as the yield strength, this kind of fatigue crack propagation resistance is indirectly dependent on the yield strength of steels.

REFERENCES

1. Paris, P. C., Gomez, M. P. and Anderson, W. E., "A Rational Analytic Theory of Fatigue," *The Trend in Engineering*, University of Washington, Vol. 13, No. 1, 1961, p. 9.
2. Paris, P. C. and Erdogan, F., "A Critical Analysis of Crack Propagation Laws," *Transactions of the ASME, Journal of Basic Engineering*, Vol. 85, 1963, pp. 528-534.
3. Swanson, S. R., Cicci, F. and Hoppe, W., "Crack Propagation in Clad 7079-T6 Aluminum Alloy Sheet Under Constant and Random Amplitude Fatigue Loading," in Fatigue Crack Propagation, ASTM Spec. Tech. Pub. No. 415, 1967, p. 312.
4. Wilhelm, D. P., "Investigation of Cyclic Crack Growth Transitional Behavior," in Fatigue Crack Propagation, ASTM Spec. Tech. Pub. No. 415, 1967, p. 363.
5. Schijve, J., "Significance of Fatigue Cracks in the Micro-range and Macro-range," in Fatigue Crack Propagation, ASTM Spec. Tech. Pub. No. 415, 1967, p. 415.
6. J. M. Barsom, "Fatigue-Crack Propagation in Steels of Various Yield Strengths," presented at the First National Congress of Pressure Vessels and Piping, San Francisco, California, May 10-12, 1971.
7. Liu, H. W., "Fatigue Crack Propagation and Applied Stress Range -- An Energy Approach," *Transactions of the ASME, Journal of Basic Engineering*, Vol. 85, No. 1, 1963, pp. 116-122.
8. Liu, H. W. and Iino, N., "A Mechanical Model for Fatigue Crack Propagation," *Proceedings of the 2nd International Conference on Fracture*, Paper No. 71, Published by Chapman and Hall, 1969, pp. 812-823.
9. Tomkins, B., "Fatigue Crack Propagation - An Analysis," *Philosophical Magazine*, Vol. 18, 1968, pp. 1041-1066.
10. Dugdale, D. S., "Yielding of Steel Sheets Containing Slits," *Journal of the Mechanics and Physics of Solids*, Vol. 8, 1960, pp. 100-104.
11. Hickerson, J. P. Jr., and Hertzberg, R. W., "The Role of Mechanical Properties in Low Stress Fatigue Crack Propagation," *Metallurgical Transactions*, Vol. 3, Jan., 1972, pp. 179-189.
12. McClintock, F. A., "On the Plasticity of the Growth of Fatigue Cracks," in Fracture of Solids, edited by Drucker and Gilman, published by Wiley, 1963, pp. 65-102.
13. Rice, J. R., "Mechanics of Crack Tip Deformation and Extension by Fatigue," in Fatigue Crack Propagation, ASTM Spec. Tech. Pub. No. 415, 1967, p. 247.

14. Neuber, H., "Theory of Stress Concentration for Shear Strained Prismatical Bodies with Arbitrary Non Linear Stress-Strain Law," Transactions of the ASME, Journal of Applied Mechanics, Vol. 28, 1961, pp. 544-550.
15. Weiss, V., "Analysis of Crack Propagation in Strain Cycling Fatigue," in Fatigue - An Interdisciplinary Approach, edited by Burke, Reed and Weiss, Syracuse University Press, 1964, pp. 179-186.
16. Fleck, W. G. and Anderson, R. B., "A Mechanical Model of Fatigue Crack Propagation," Proceedings of the 2nd International Conference on Fracture, Paper No. 69, Published by Chapman and Hall, 1969, pp. 790-802.
17. Fleck, W. G. and Anderson, R. B., "A Model of the Characteristics of Fatigue Crack Extension," Proceedings of the Air Force Conference on Fatigue and Fracture of Aircraft Structures and Materials, Miami Beach, Florida, 1969, pp. 417-424.
18. Rice, J. R., "Stresses Due to a Sharp Notch in a Work Hardening Elastic Plastic Material Loaded by Longitudinal Shear," Brown University Tech. Report NSF GK-286/1, Dec., 1965.
19. Gurland, J., "Correlation between Yield Strength and Microstructure of Some Carbon Steels," in Stereology and Quantitative Metallography, ASTM Spec. Tech. Pub. No. 504, 1972, pp. 108-118.
20. Landgraf, R. W., "The Resistance of Metals to Cyclic Deformation" in Achievement of High Fatigue Resistance in Metals and Alloys, ASTM Spec. Tech. Pub. No. 467, 1970, pp. 3-36.

Table I Reported (6) and Estimated Mechanical Properties of the Steels (1)

Material	Values Reported by Barsom(6)				Estimated Cyclic Properties (2)			
	Ultimate Strength ksi	0.2% Offset Yield Strength, ksi	% Red. in Area	n'	ϵ'_f	c	σ'_f ksi	b
HY 80	113	95	70	0.12	1.25	-0.65	163	-0.080
HY 130	148	140	67	0.12	1.15	-0.65	198	-0.080
10 Ni-Cr-Mo-Co	193	182	71	0.12	1.25	-0.65	243	-0.080
12 Ni-5Cr-3Co	187	184	64	0.12	1.00	-0.65	237	-0.080
A36	75	36	68	0.14	1.15	-0.60	125	-0.085
ABS-C	63	39	66	0.14	1.10	-0.60	113	-0.085
A302-B	88	56	67	0.14	1.10	-0.60	138	-0.085
A537-A	83	59	73	0.14	1.30	-0.60	133	-0.085

(1) Modulus of Elasticity was taken as 30,000 ksi for all steels.

(2) $n' \approx 0.12$ and $c \approx -0.65$ were used for the four harder steels while $n' \approx 0.14$ and $c \approx -0.60$ were used for the softer steels; b was approximated as $b = n'c$; ϵ'_f was approximated as the true fracture ductility which is defined as $\epsilon'_f \approx \ln[100/(100 - \%RA)]$; σ'_f was estimated by adding 50 ksi to the ultimate strength. These techniques for estimating the cyclic properties have been employed for a number of years at Illinois and elsewhere when only the ordinary tensile properties of a steel are known. See, for example, Ref. (20). Actual test data would, of course, be preferable to such crude estimates. Potential errors in the estimated properties, however, will have a relatively small effect on the calculated crack propagation resistance (See Fig. 5).

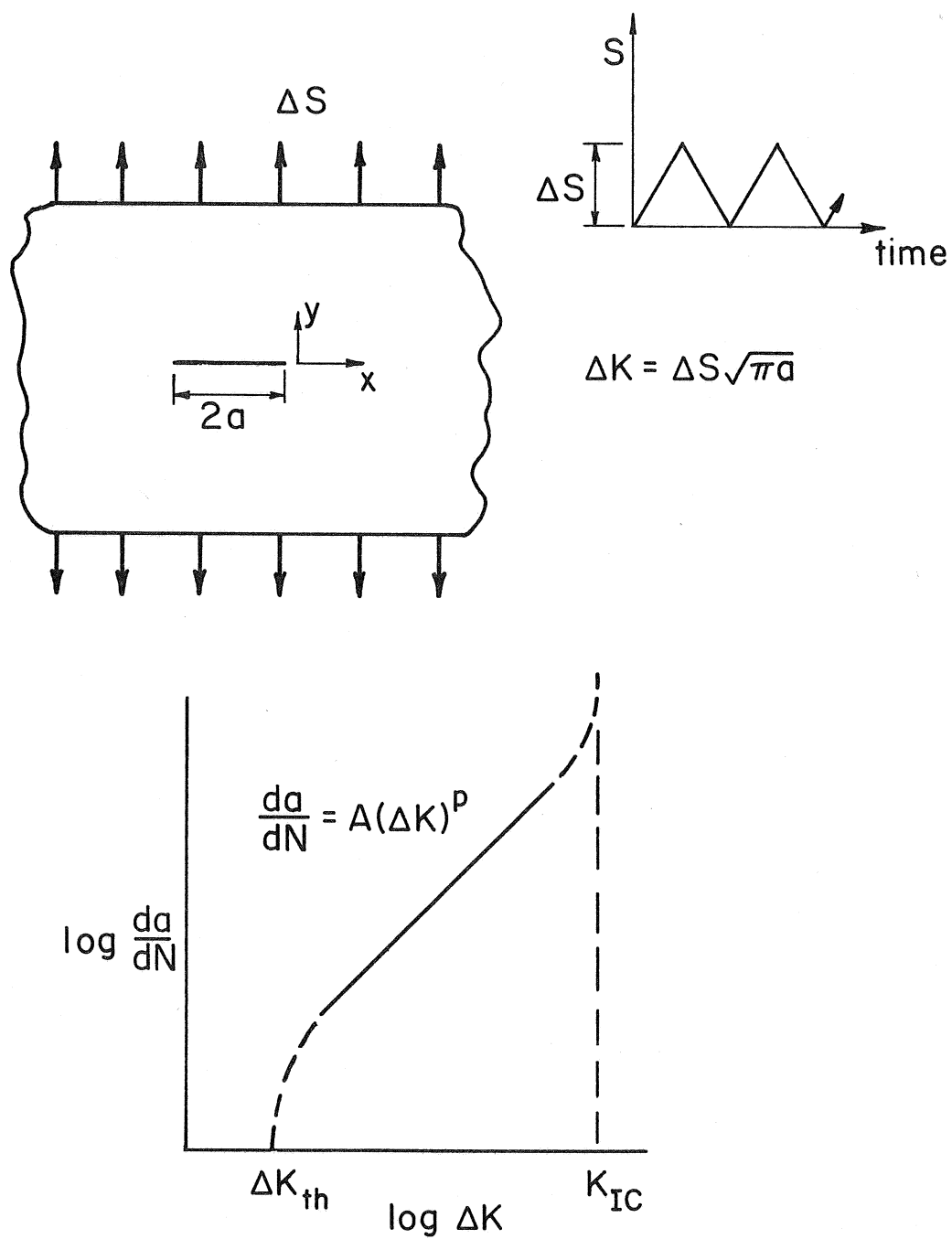


Fig. 1 DEFINITION OF TERMS AND TYPICAL CRACK PROPAGATION DATA

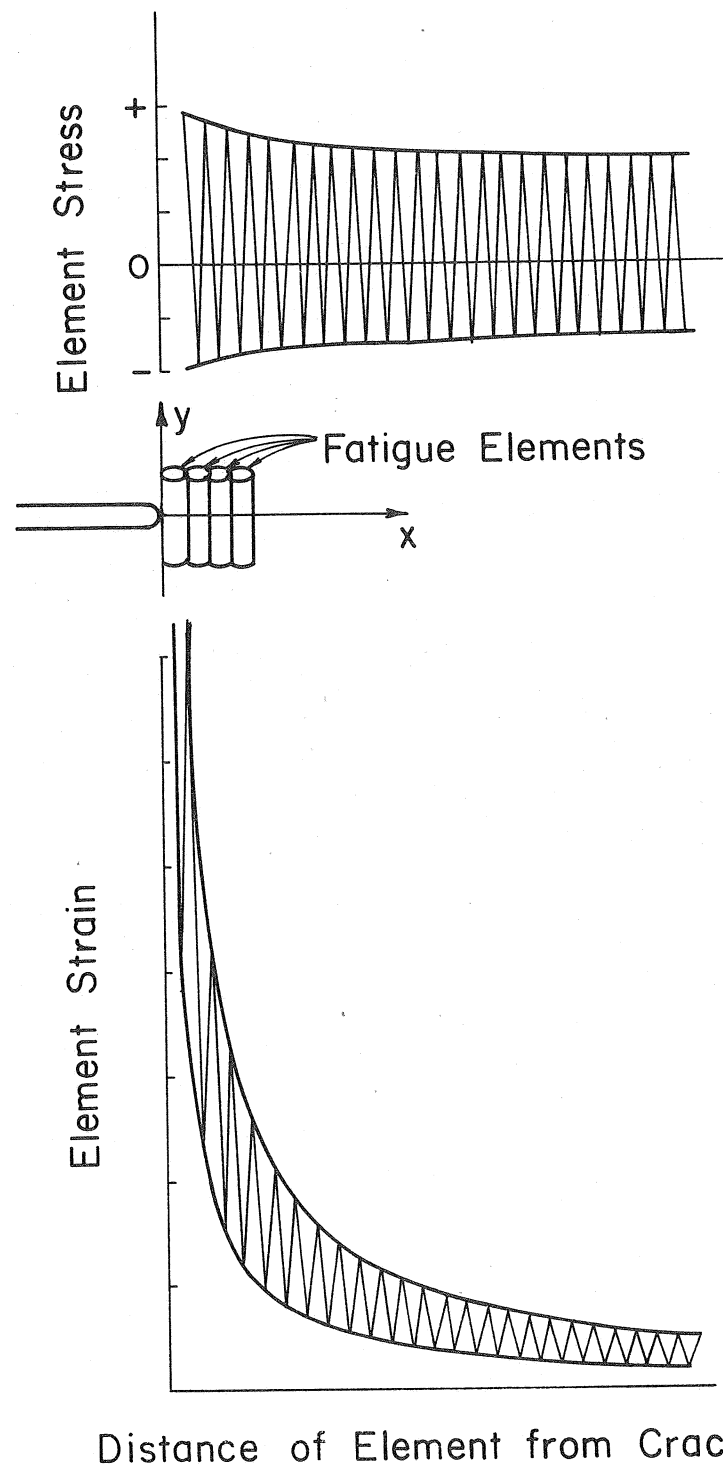
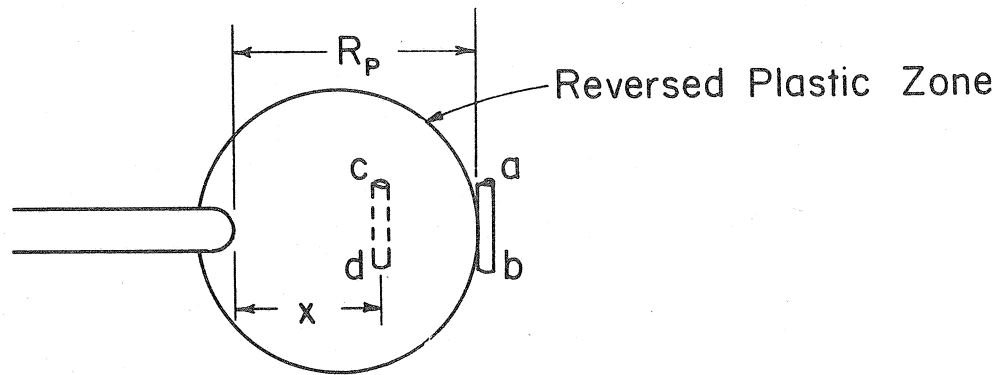
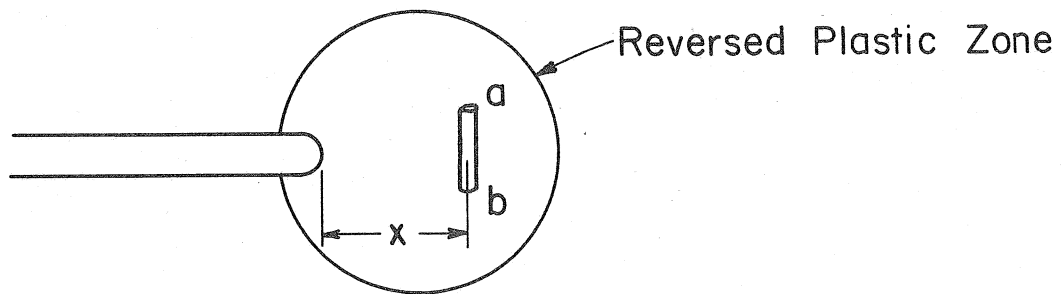


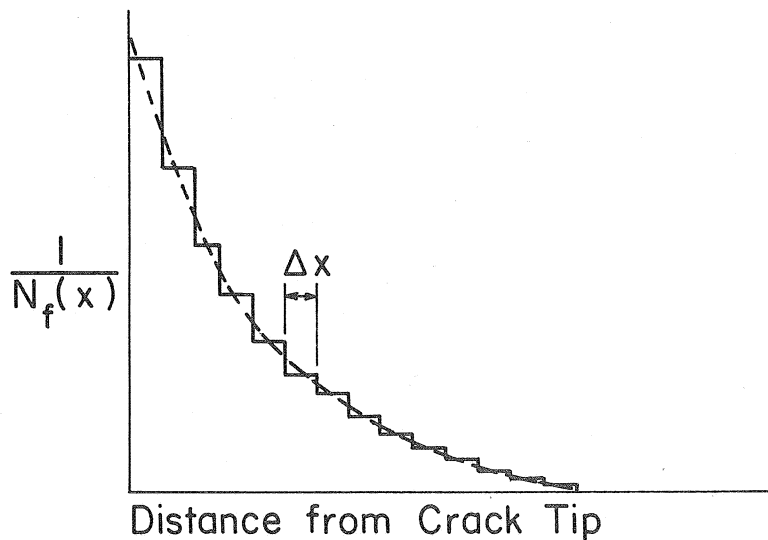
Fig. 2 SCHEMATIC OF STRESS-STRAIN HISTORY OF A FATIGUE ELEMENT AHEAD OF THE CRACK TIP



(a) ELEMENT AT EDGE OF REVERSED PLASTIC ZONE



(b) ELEMENT AT DISTANCE x FROM CRACK TIP



(c) DAMAGE HISTORY OF AN ELEMENT

Fig. 3 TYPICAL DAMAGE HISTORY OF AN ELEMENT

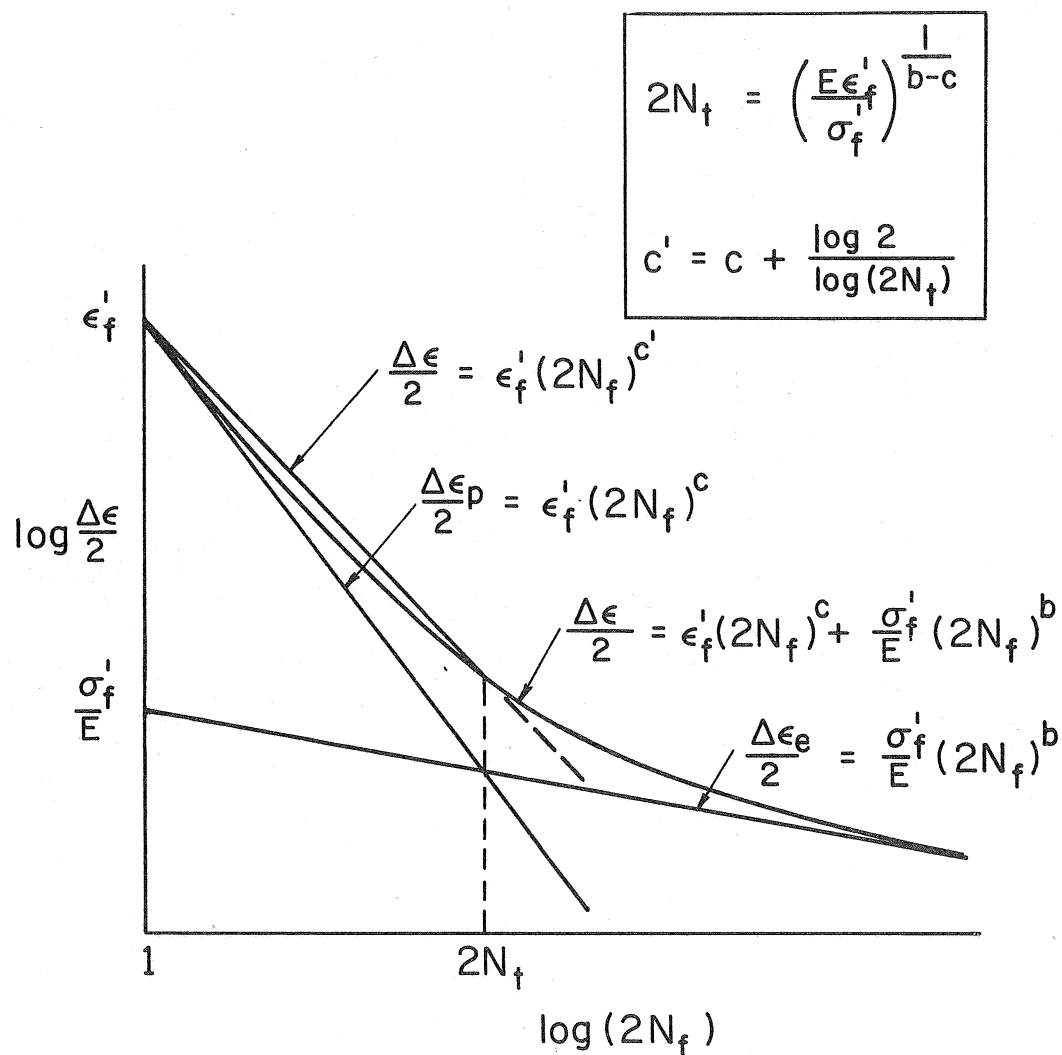


Fig. 4 APPROXIMATING TOTAL STRAIN AMPLITUDE
VERSUS LIFE PLOTS BY POWER FUNCTIONS

Reference Values of the Variables

$$\begin{array}{lll} \epsilon_f' = 1 & n' = 0.15 & \\ \sigma_f' = 150 \text{ ksi} & b = -0.09 & \\ \sigma_y' = 60 \text{ ksi} & c = -0.60 & \end{array}$$

$$E = 30,000 \text{ ksi}$$

$$A_{\text{ref}} = 2 \times 10^{-8} \text{ ksi}^{-2}$$

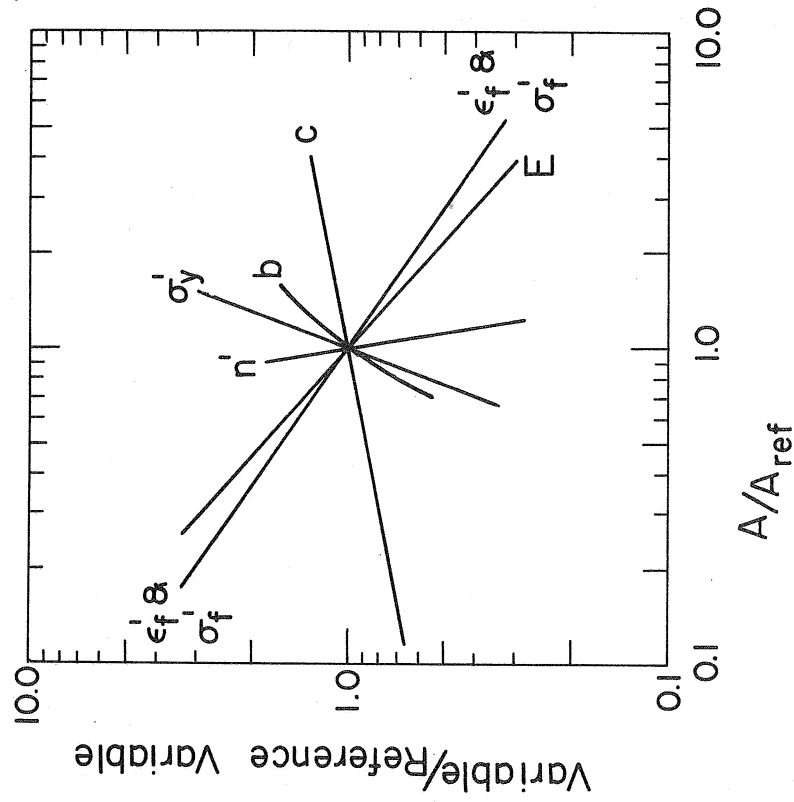


Fig. 5. EFFECT OF MATERIAL PROPERTIES ON COEFFICIENT A OF EQ.(13)

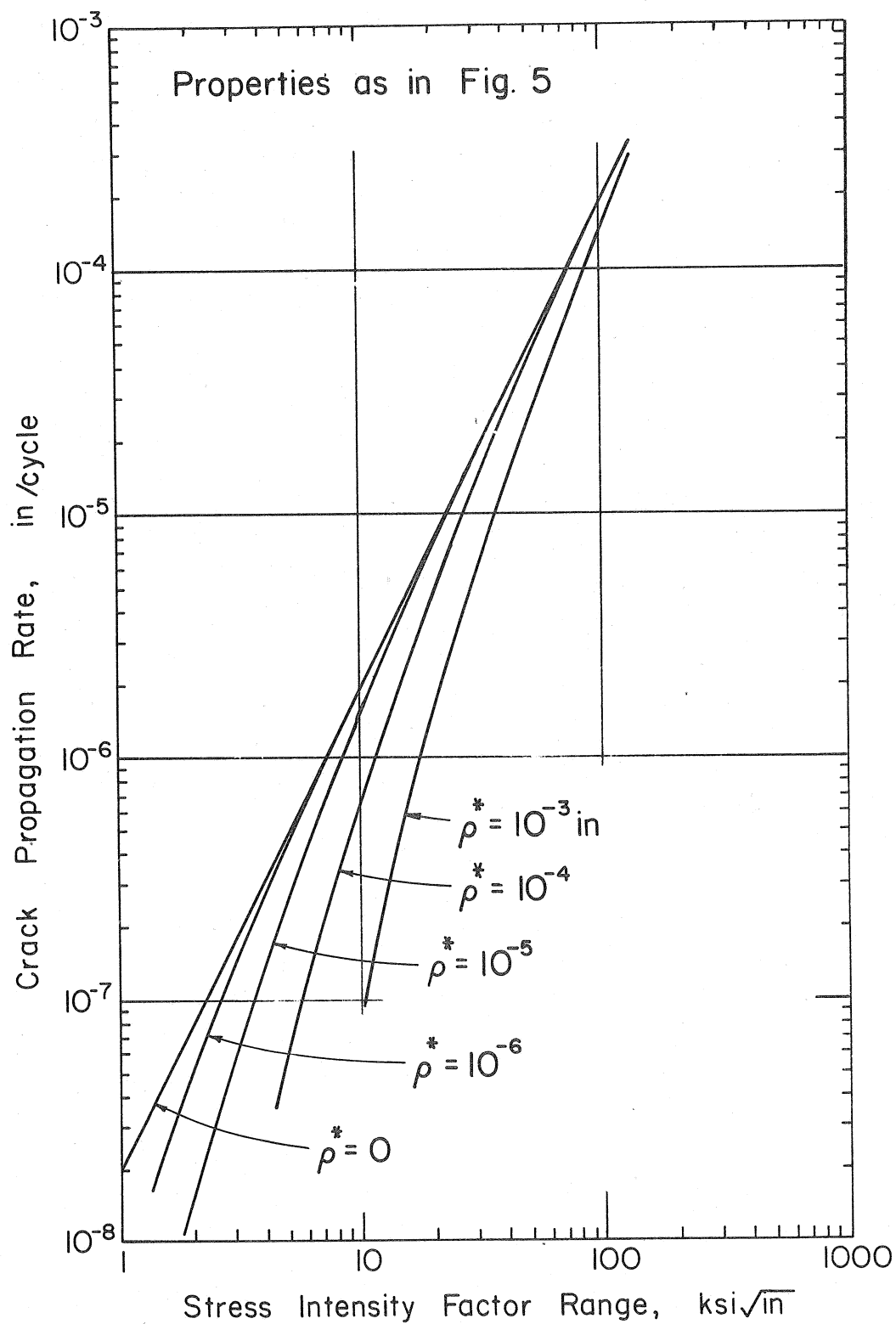


Fig. 6 EFFECT OF MICROSTRUCTURE SIZE ON FATIGUE CRACK PROPAGATION RATE

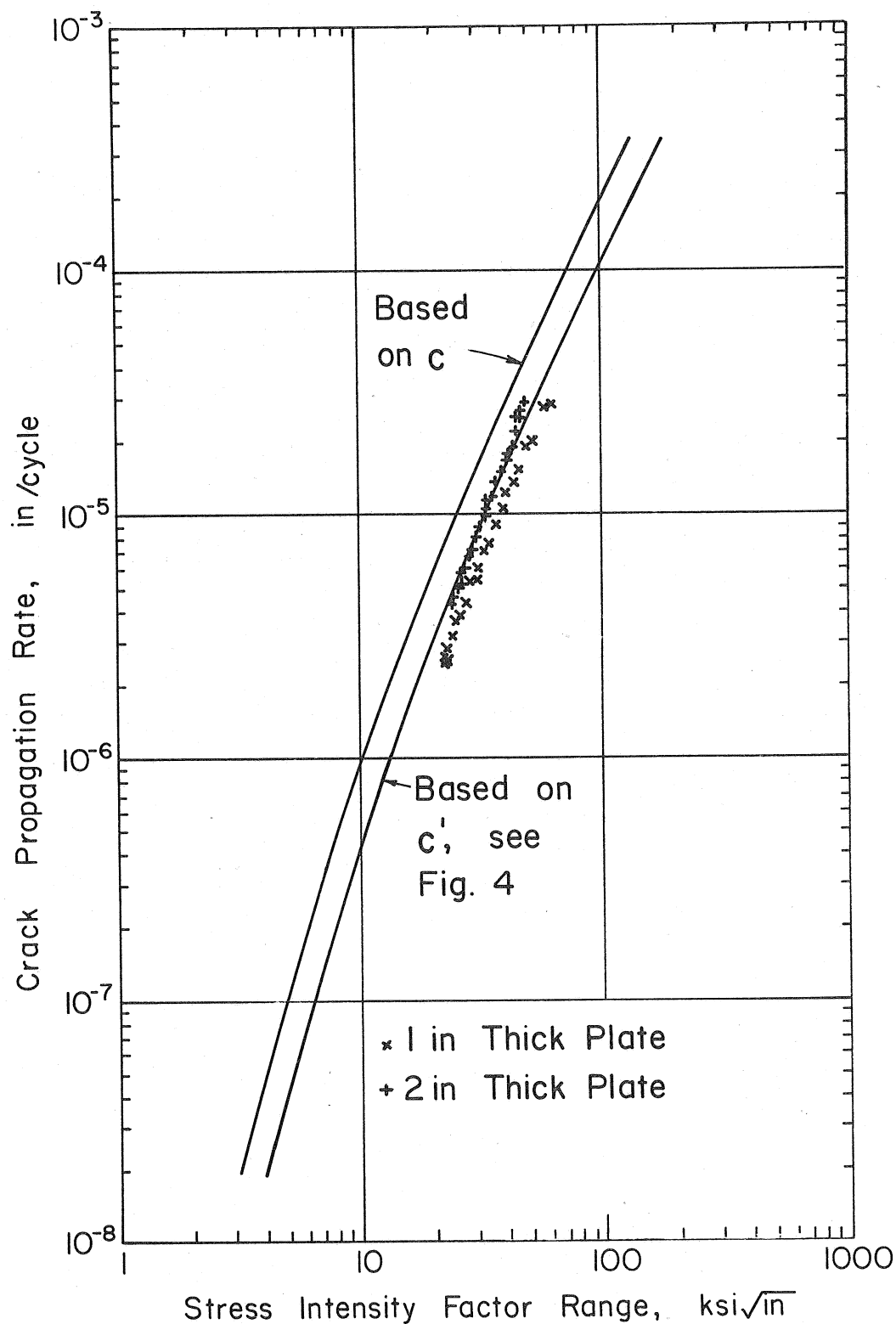


Fig. 7 COMPARISON OF EXPERIMENTAL DATA(6) WITH THEORETICAL PREDICTION FOR HY-80 STEEL

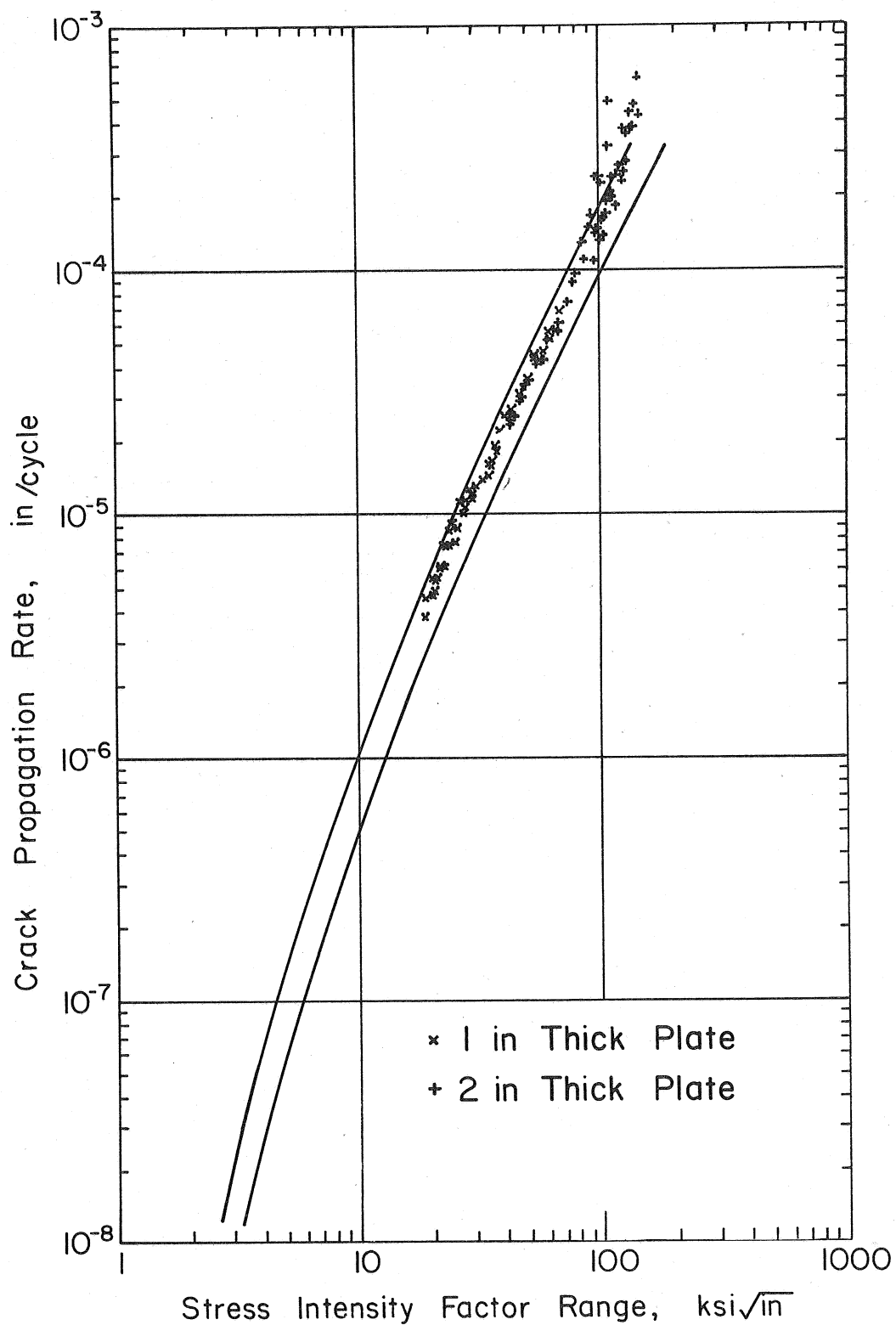


Fig. 8 COMPARISON OF EXPERIMENTAL DATA(6) WITH THEORETICAL PREDICTION FOR HY-130 STEEL

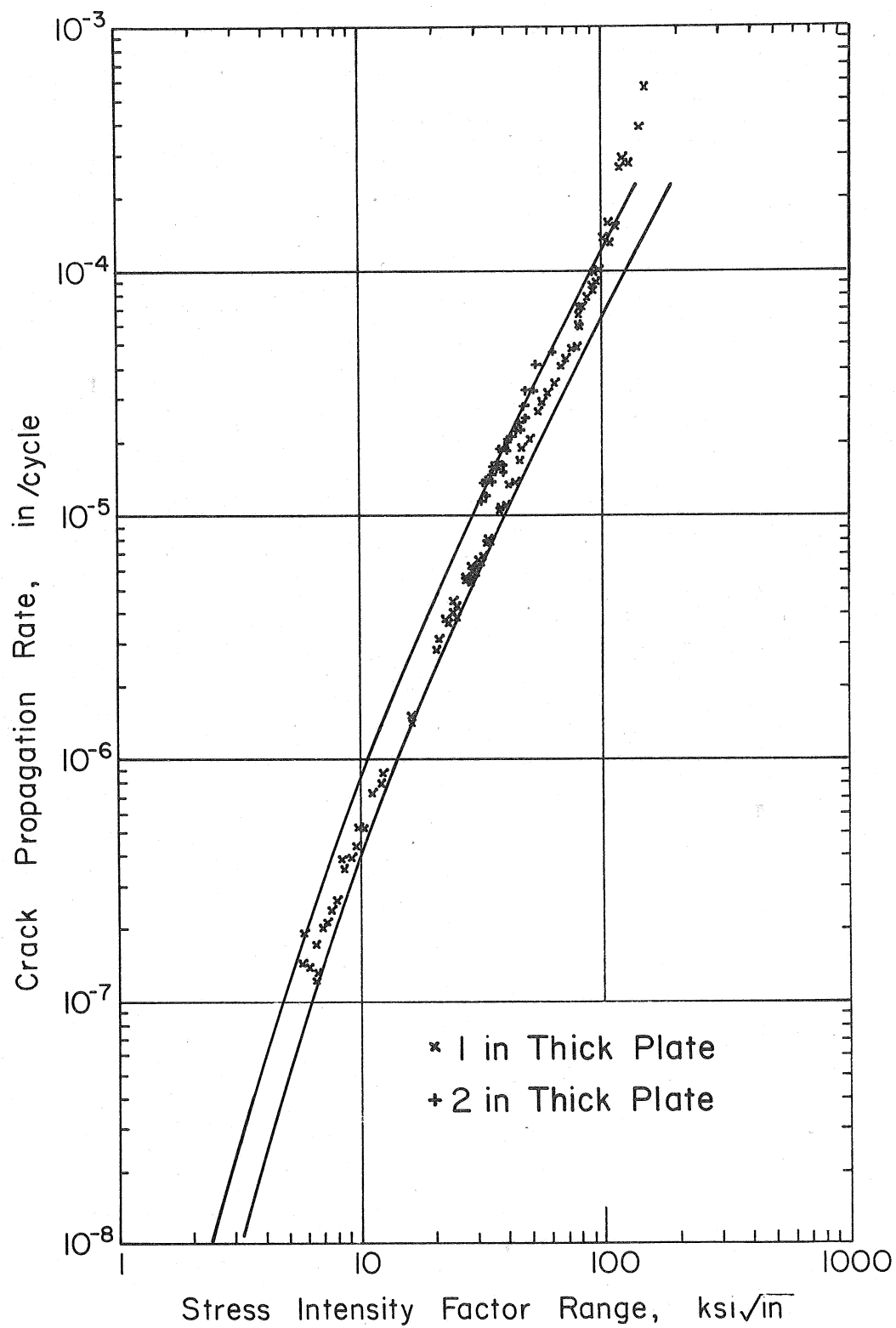


Fig. 9 COMPARISON OF EXPERIMENTAL DATA(6) WITH THEORETICAL PREDICTION FOR IONi-Cr-Mo-Co STEEL

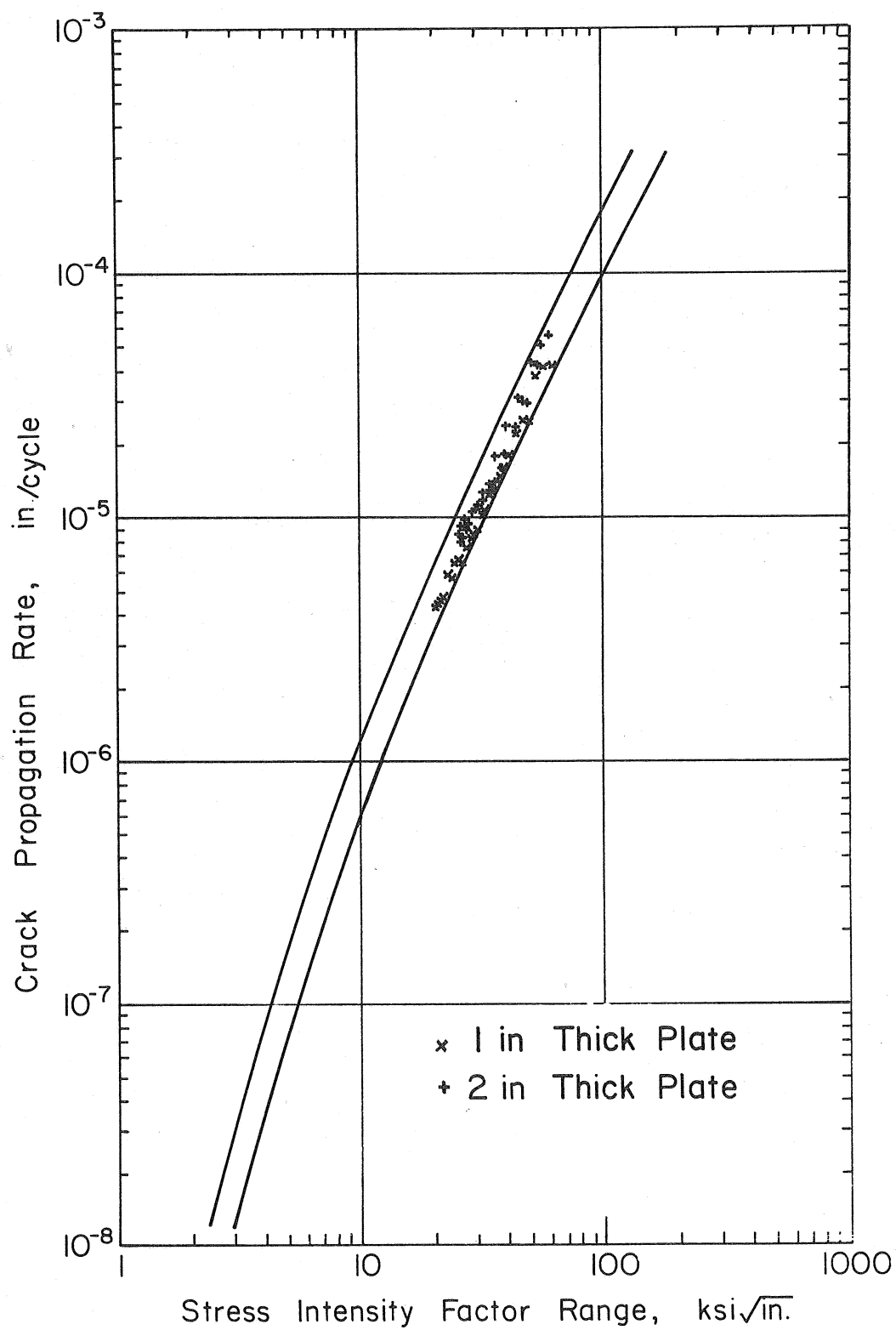


Fig. 10 COMPARISON OF EXPERIMENTAL DATA(6) WITH THEORETICAL PREDICTION FOR 12Ni-5Cr-3Co STEEL

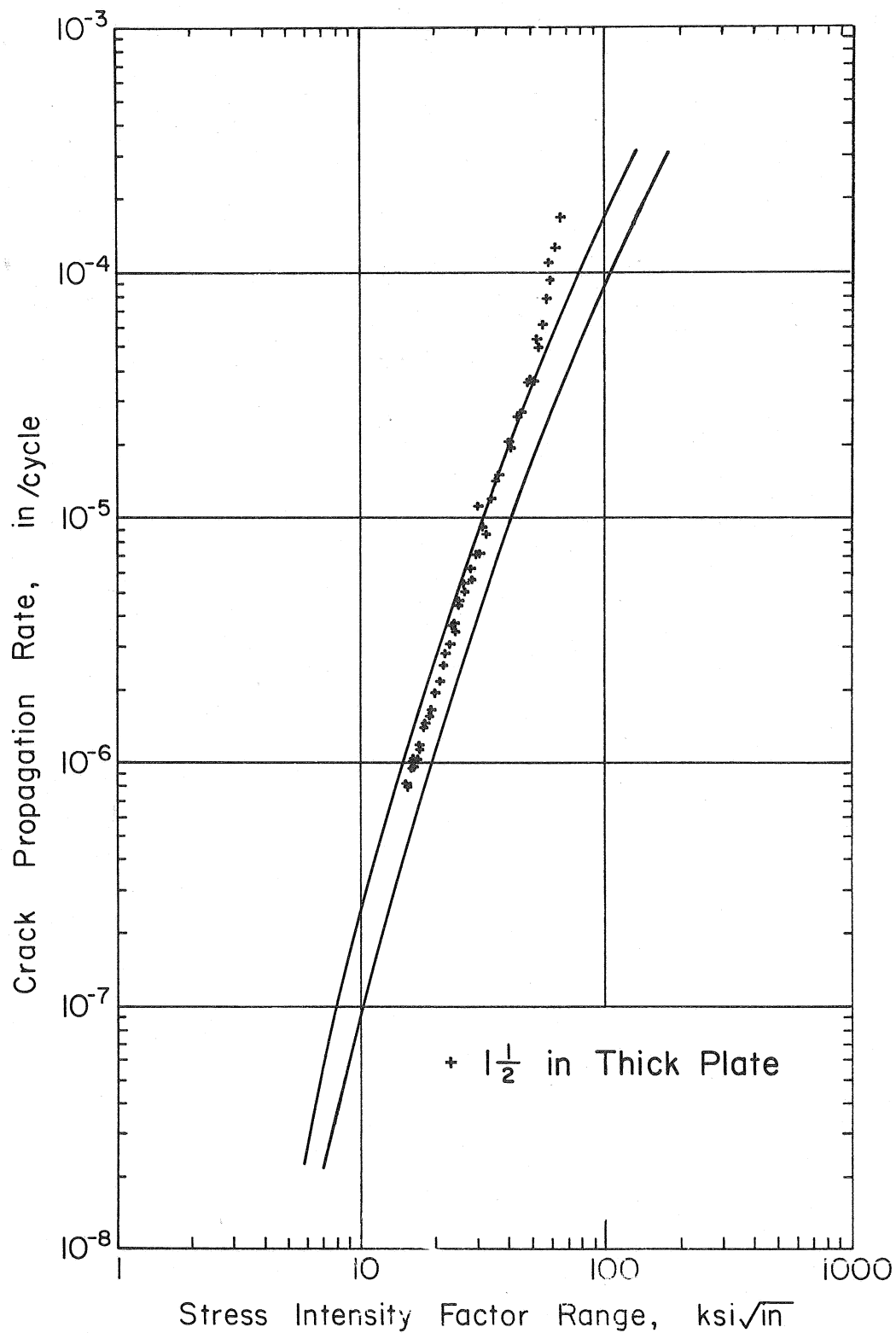


Fig. II COMPARISON OF EXPERIMENTAL DATA(6) WITH THEORETICAL PREDICTION FOR A36 STEEL

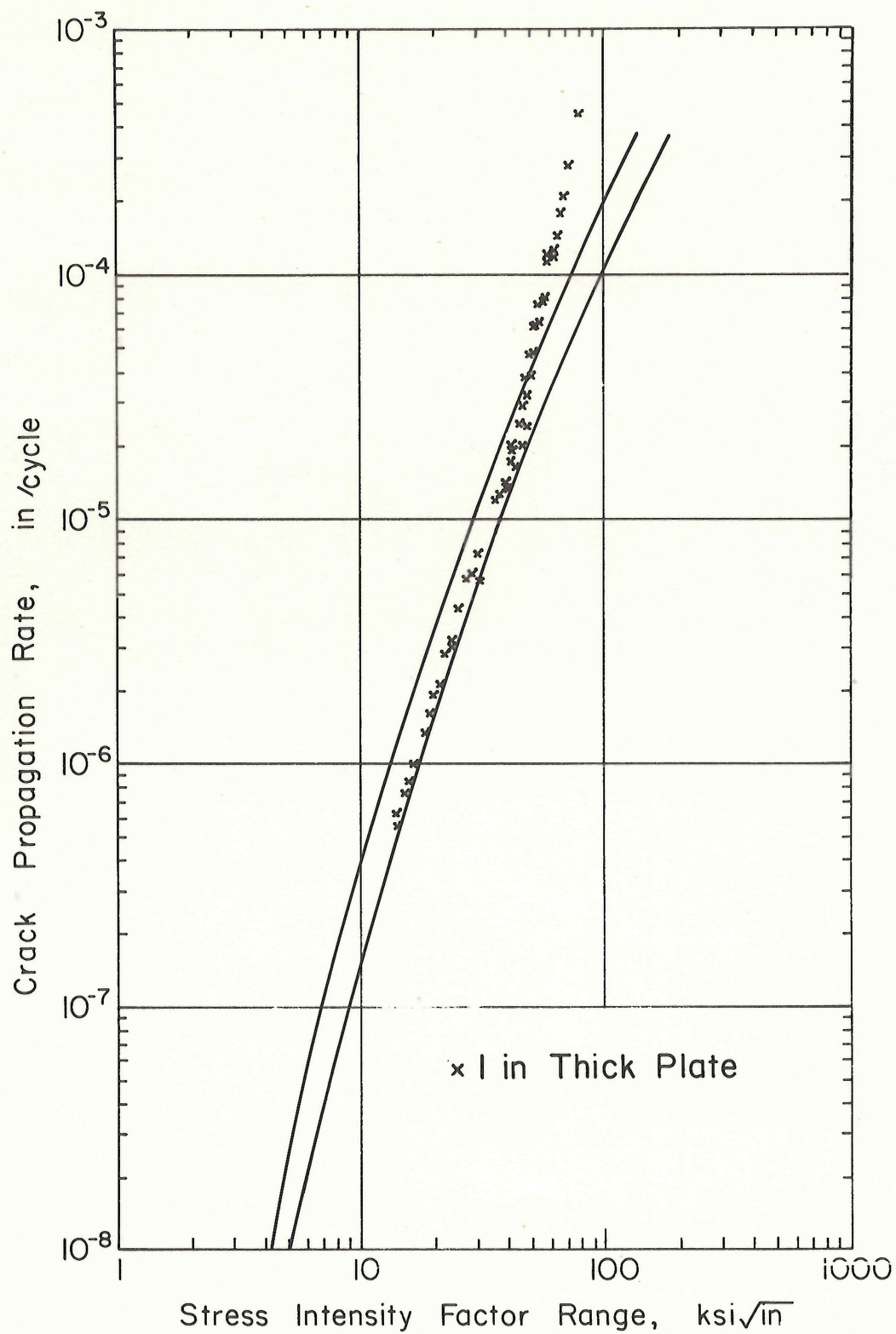


Fig. 12 COMPARISON OF EXPERIMENTAL DATA(6) WITH THEORETICAL PREDICTION FOR ABS-C STEEL

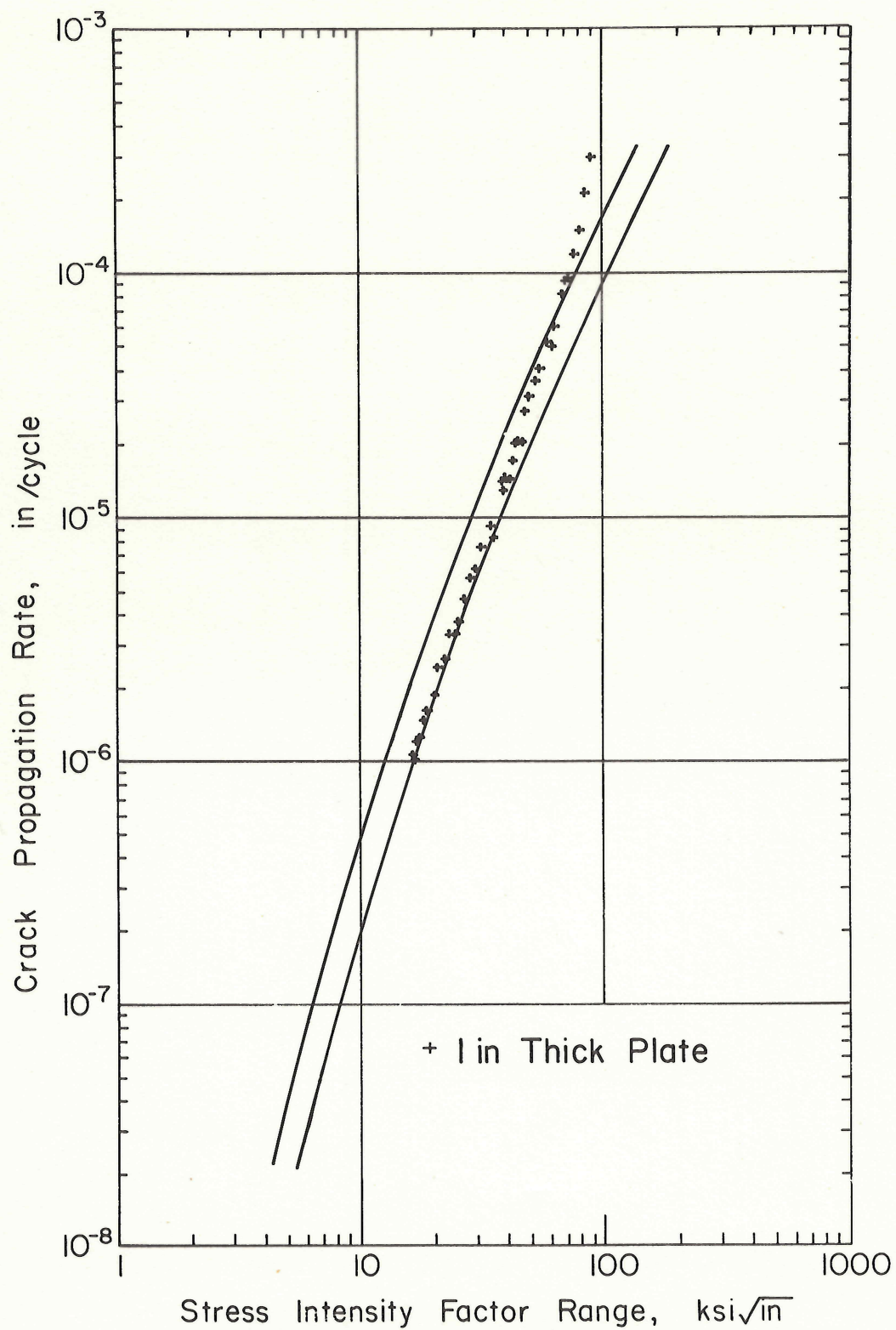


Fig. 13 COMPARISON OF EXPERIMENTAL DATA(6) WITH THEORETICAL PREDICTION FOR A302-B STEEL

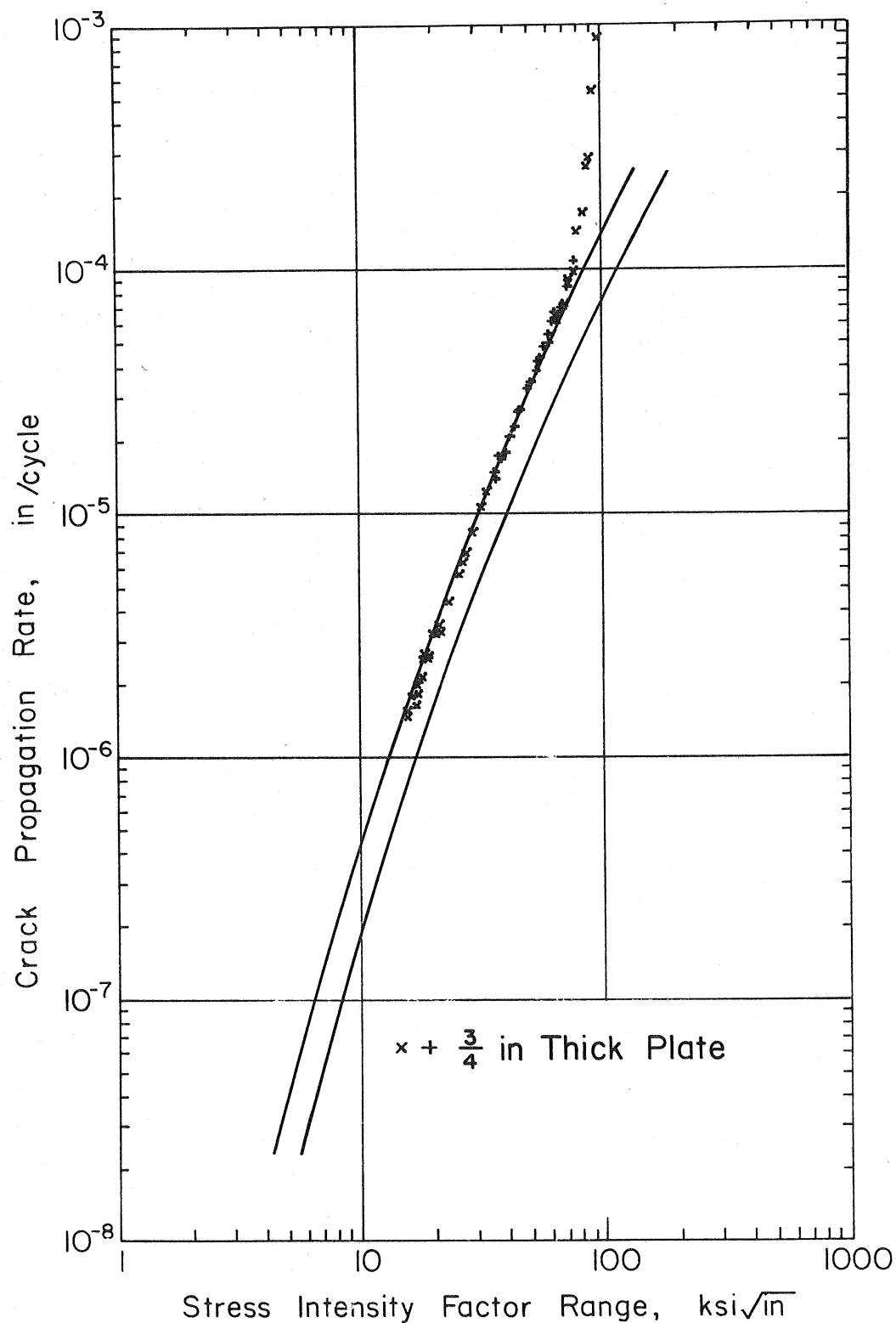


Fig. 14 COMPARISON OF EXPERIMENTAL DATA(6) WITH THEORETICAL PREDICTION FOR A537-A STEEL